FDD algorithm for an AHU reverse-return system

Natasa Djuric Vojislav Novakovic
Postdoctoral fellow Professor
Norwegian University of Science and Technology (NTNU), Department of Energy and Process Engineering
Trondheim, Norway

ABSTRACT

A fault detection and diagnosis (FDD) algorithm was developed for an AHU reverse-return system for air cooling. These FDD rules were generated using simulation in three steps. Cause-effect rules were established by connecting the faults and their related effects. The FDD rules were developed for the following faults: old valve, fouled return pipe, fault in the outlet air temperature sensor, fault in the temperature sensor for the inlet temperature, bad position of the sensor for pressure difference. The effects of the involved faults were observed on four system performances. The results showed that increase in both the cooling coil rate and the pump rate appear due to faults in sensors. The inaccurate measurement of the pressure difference and the fault in the control valve do not affect the AHU outlet air temperatures. Increase in both the outlet air temperature and the pump power consumption appears due to the fouled return pipes.

Key words: performance, performance index, fault detection and diagnosis, air-handling unit

1 INTRODUCTION

There is an increasing realization that many buildings do not perform as intended by their designers. Reasons include faulty construction, malfunctioning equipment, incorrectly configured control systems, and inappropriate operating procedures (Haves, 2001). Due to abnormal physical changes, ageing, or inadequate maintenance of HVAC components, HVAC components easily suffer from complete failure (hard fault) or partial failure (soft fault) (Wang and Xiao, 2004). Even though building performances are normally supervised by BEMS, when a fault occurs in the system, the BEMS programs currently available do not adequately assist in finding the underlying cause of the fault. Therefore, diagnosis of the defect is left to the operator (Hyvarinen and Karki, 1996).

There has been much interest in the development of FDD techniques that are suitable for use in building control systems. In addition, there are many different diagnosis techniques and listed faults for different HVAC systems (Hyvarinen and Karki, 1996). For example, a practical algorithm for diagnosing control loop problems in an AHU was provided by Salsbury and Diamond (1999). Deviations in the indoor air temperature and energy consumption caused by different faults were explained practically, using an easy-to-use tool for FDD in (Song et al., 2008). A method for the AHU sensor fault detection based on the principal component analysis (PCA) was elaborated in the work of Wang and Xiao (2004). Two types of faults, an open window and a defective radiator valve, were studied using the model-based FDD in (Yu et al., 2003). An on-line diagnostic test, which diagnoses distinct and abrupt faults in an AHU, was directly programmed in the building automation system in (Pakanen and Sundquist, 2003).

Comparison of the expected and deviated performance is fault detection, while diagnosis means fault identification. Therefore, different FDD tools have diversity in the fault classifiers used. A fault classifier is a way faults are diagnosed. Difference between the expected and deviated performance can be expressed by an index. An index can have a different background depending on the method. For example, FDD applications of the PCA method use the squared sum of the residual, named the Q-statistic or squared prediction error (SPE), as an index of faulty conditions. Consequently, the Q-contribution plot can be used to diagnose the fault. The variable making a large contribution to the Q-statistic or SPE is indicated to be the potential fault source (Wang and Xiao 2004). Similarly, in this study performance indices (PI) were involved for fault diagnosis. These performance indices measure a bias in a building performance in the case when a fault appears. Consequently, based on a positive or negative threshold bias of the PIs, the cause-effect rules for fault diagnosis were developed.

Since the aim of this study was to develop cause-effect rules for fault diagnosis, five operation faults were tested. Finally, the cause-effect rules for these faults were developed. The PIs were calculated for two air outlet temperatures, coil cooling rate, and the pump power. This study was carried out on the platform presented in (Wang and Xinhua 2007).

2 SYSTEM DESCRIPTION

This system description introduces the AHU air cooling system and implemented thermal load. This system was developed for the second zone of the super high-rise located in Hong Kong (Ma et al., 2008).

The hydronic system for AHUs for air cooling is a reverse-return system. The schematic diagram of these AHUs connected in the reverse-return system is shown in Figure 1. The AHUs are connected by pipes, while the control valve controls the water flow through each AHU. In this case, the dynamic balance valve (DBV) at the return side of the cooling coil was not included in the system. Therefore, each parallel branch is the same, with an AHU and a control valve.

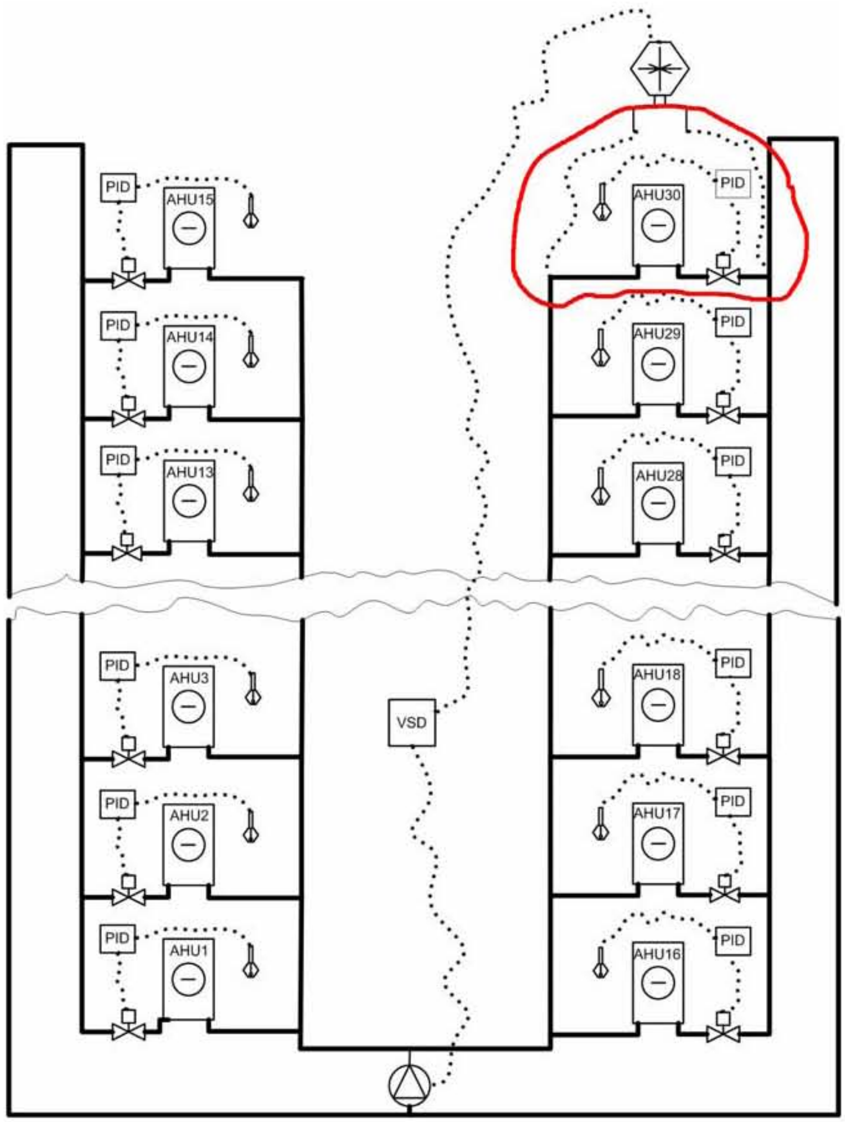

Figure 1. Schematic diagram of the reverse-return system for AHUs

In a reverse-return approach, the first coil supplied is the last returned and vice versa. In such a system, differential pressure across each coil remains fairly constant. The circulation water pump has a variable speed drive (VSD) controlled by a differential pressure sensor located across the riser taps at the most remote AHU, the one marked in Figure 1.

The valve position of AHU is controlled by the PID controller output. So based on the cooling loads and the system status schedule of each coil, the PID controller opens the AHU valves. The PID pump controller uses the pressure difference on the most remote AHU, to find the pump frequency. As the pressure difference is increasing due to high water flow, the pump head is higher.

The described system was observed during the working hours. The cooling load profile and the outdoor air temperature for these hours are shown in Figure 2. Such a load profile has been obtained from a previous study based on (Xu et al., 2008). In addition, there is an assumption that the cooling loads are the same for all the AHUs. So, the cooling load in Figure 2 is divided equally to each AHU. The regime for using the AHUs is the following: from 8 a.m. to 9 p.m. all the AHUs are in use, while outside of this time, 10 AHUs are in use.

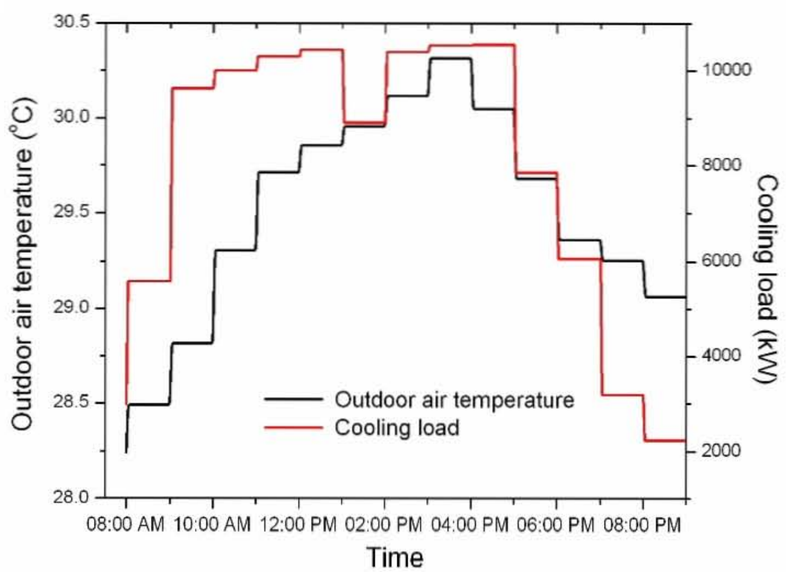

Figure 2. Outdoor air temperature and the cooling load profile of the AHU system

3 METHOD

3.1 The Fault Effect Assessment and Performance Indices

To estimate the effects of the faults, the performance indices were involved. PI can help to detect a fault. These performance indices measure a bias in a building performance in the case when a fault appears. A performance index is defined as the percent difference between a faulty performance and a correct performance. Therefore, the baseline for the PI calculation is defined to be a correct performance, or a system state without faults. To diagnose a fault, cause-effect rules have been established based on the performance indices values and the indices combination, which gives a certain fault. If a PI value is above the positive threshold, or under the negative threshold, then such a PI is labeled. A combination of these PI labels gives a rule for fault diagnosis.

A general form of a performance index can be written as

$$PI_E = \frac{E_{actual} - E_{no\_fault}}{E_{no\_fault}} \times 100 \,, \qquad (1)$$

where E_{actual} is an actual building performance when there might be a fault in the system, and E_{no_fault} is the building performance when there is no fault in the system. Equation 1 can be used to calculate different performance indices, such as for energy consumption or pump power. If there is a set-point value of a performance index, then such an index is defined as

$$PI_E = \frac{E_{actual} - E_{set}}{E_{set}} \times 100 \,, \qquad (2)$$

where E_{set} is the set-point value of a performance E. The performance index defined by Equation 2 can be used for a performance such as the indoor air temperature. In the case of calculation of PI for the temperature, the temperature was expressed in the Celsius degree scale (^oC).

In a case when $E_{no\_fault}=0$ or $E_{set}=0$, while $E_{actual}\neq 0$, Equations 1 and 2 are not defined. To get a continuous calculation of the suggested method, an algorithm was suggested. The algorithm is:

if $E_{no\_fault}=0$ or $E_{set}=0$ and $E_{actual}>0$
then PI is equal to a chosen positive threshold;
if $E_{no\_fault}=0$ or $E_{set}=0$ and $E_{actual}<0$
then PI is equal to a chosen negative threshold;

After the performance indices have been calculated, rules for fault diagnosis can be developed. Before the rules are developed, three terms are necessary. These terms are:

- When a $PI_E\geq 10\%$, then that index is called a positive index and is labeled P.
- When a $PI_E\leq -10\%$, then that index is called a negative index and is labeled N.
- When $-10\leq \%PI_E\leq 10\%$, then that index gets the label NF.

The threshold of ±10% has been suggested for the purpose of this study. For example, in a diagnostic agent for building operation (DABO, 2007), which is a software tool running in the central building operator station, this threshold for the fault detection is ±8%. DABO uses expert knowledge to identify faults through the use of a hybrid knowledge-based system composed of an Expert System and a Case-Based Reasoning module. Haves and Khalsa (Haves and Khalsa, 2000) suggested a threshold for fault detection of 15%, in the case that the baseline model is deemed to be a correct operation. In the case when the model is based on faulty operation, then the threshold could be set to about 7% (Haves and Khalsa, 2000). Regardless of the threshold value, the most important issue for the performance indices labeling is their positive or negative bias.

The logical rules for the fault diagnosis have been developed based on how many and which performance indices have N, P or NF as labels. For example, if all the observed PIs have the labels NF, then there is no fault in the system, or a fault cannot be detected by using these indices.

Finally, the FDD rules were established in three steps: testing different faults, calculating the performance indices (PI) using Equations 1 and 2, and classifying the observed PIs using the above labeling system.

3.2 Fault Description

To establish rules for the FDD in the reverse-return AHU system, it was necessary to test the system performances on a few possible faults. Therefore, the faults are explained first, and then tested.

Old valve

Due to ageing, the control valve cannot achieve the same position as the signal from the valve controller indicates. In that case, the control valve is not opened as the coil PID controller signals. For example, the valve may be opened more in reality than it should be according to the PID controller. Since it is not possible to measure the actual control valve position, this fault can be identified by checking the valve controller signal and the resulting controlled temperature. If the control valve does not have the same position as the signal from the valve controller, then the valve position signal from PID is very low and the controlled temperature has many high oscillations.

Such a fault was involved in the model by biasing the input from the coil PID to the control valve.

Fouled return pipe fault

This fault can appear due to system ageing and use of poor water quality in the hydronic system. In addition, such a fault can appear in a new system due to metal particles after pipe welding. Such a fault means that the flow resistance of the pipes is increased. If the flow resistance of the return pipe is increased, then the desired outlet air temperature of AHU cannot be achieved.

This fault was involved by increasing the flow resistance coefficient (expressed in $Pa/(m^3/s)^2$) of the pipes in the return branches.

Fault in the outlet air temperature sensor

The outlet air temperature sensor measures the air temperature after the AHU, actually, after the cooling coil. Sometimes this sensor for the coil outlet air temperature can be placed on the wrong place or due to ageing of the sensor the temperature measurement can be incorrect. If the sensor for the coil outlet air temperature measures an incorrect temperature, then it influences the control loop for the outlet air temperature. Therefore, the control will be poor and the system will perform poorly.

This fault was involved by biasing the coil PID controller input from the AHU output by +20%. This bias was added to the temperature expressed in the Celsius degree scale (^{o}C).

Fault in the temperature sensor for the inlet air temperature

The inlet air temperature measurement does not influence any control loop. A bias in the inlet air temperature sensor, however, can be influenced by taking the inlet air flow that is not the same as the real ambient air. For example, if there is an obstacle, or energy source, in front of the inlet AHU damper, then the AHU is taking air with the increased outdoor air temperature.

This fault was involved by biasing the inlet air temperature by +20%. As the previous fault, this bias was added to the temperature expressed in the Celsius degree scale (^{o}C).

Bad position of the sensor for pressure difference

The position of the pressure difference sensor is important in the direct-return system, and this sensor must be located at the most remote AHU. Such a position is also recommended for the reverse-return system. The sensor for the pressure difference can measure an incorrect pressure difference, and some of the control valves will not get correct water flow to achieve the set-point outlet air temperature. This fault can appear in the case when the system is upgraded, while the sensor for the pressure difference is not moved to the correct place. Also, in the case of very different load distribution, some branches closer to the pump can show a higher pressure drop than in the most remote ones.

This fault was modeled by setting the pressure measurement on AHU8 instead on the most remote one, AHU30, while the load on this AHU8 is only 25% of the total load. The load is 25% on AHU1 to AHU9, while the rest have a load of 100%.

4 RESULTS

The effects of the involved faults were observed on the following system performances: the total cooling coil rate, the pump rate, the AHU1 outlet air temperature, and the AHU30 outlet air temperature.

The performance indices were calculated for the above four performances. The performance indices for the cooling rate and the pump rate were calculated based on Equation 1, while the indices for the temperatures were calculated based on Equation 2. The set-point outlet air temperature was 13^{o}C. These performance indices of the AHU hydronic system are given in Figures 3 to 7. The abbreviation TOA in the following figures means the temperature of the outlet air. So, PI_{TAO1} is the performance indices for the AHU1 outlet air temperature. PI_Q is the index for the cooling coil rate, while PI_P is the performance index for the pump rate. Even though all the PIs were calculated in the same way, PIs of the old control valve, shown in Figure 3, were difficult to present. This appeared due to the used model system is resistant to the fault in the control valve.

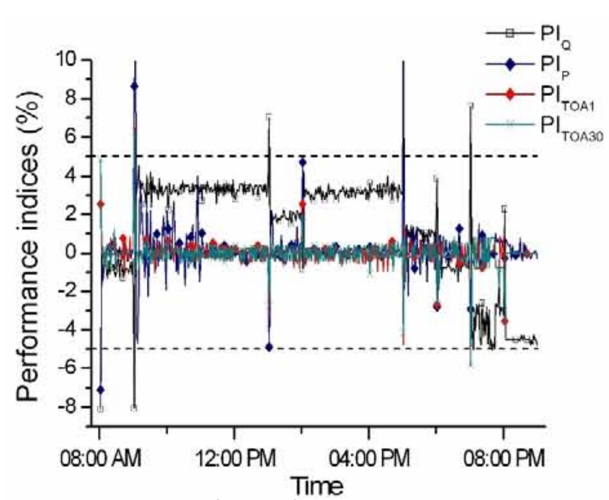

Figure 3. PIs for the fault in the control valve

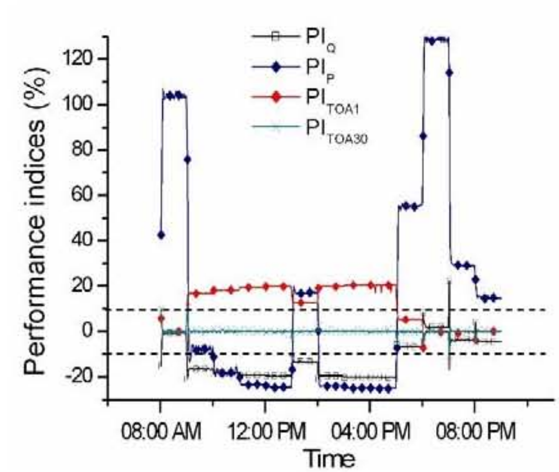

Figure 4. PIs for the fouled return pipes

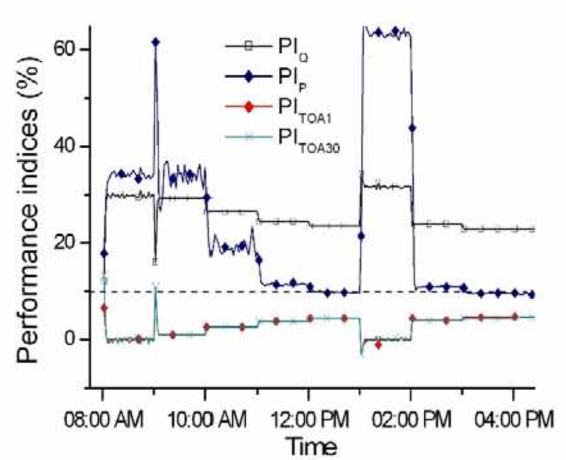

Figure 5. PIs for the fault in the inlet sensor

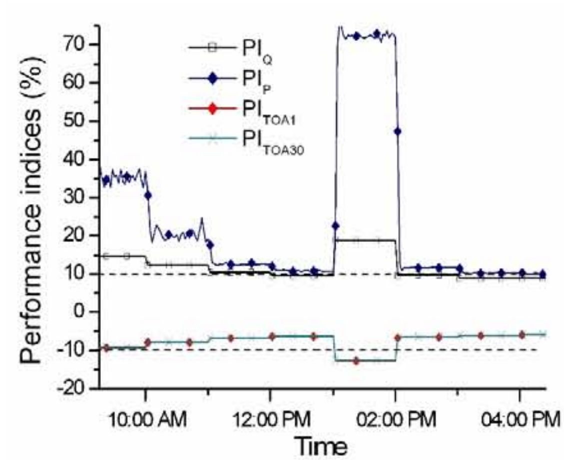

Figure 6. PIs for the fault in the outlet sensor

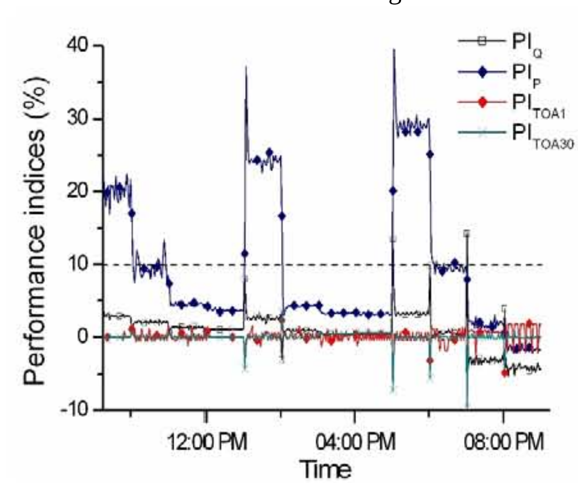

Figure 7. PIs for the fault in the measurement of Δp_{max}

In Figures 4 to 7 there are the horizontal lines at ±10% of the performance indices to show the threshold from where it can be considered that there might be a fault in the system. In Figure 3, this line is at ±5% because, in that case, there is not such a large bias in the performance indices.

5 DISCUSSIONS

The results in Figure 3 show that the observed system is quite resistant to the fault in the control valve, while more oscillations in the achieved air temperature can appear. In the case of the incorrect measurement of the pressure difference, Figure 7, it is shown that this reverse-return system is self-balanced, because regardless of the different load distribution, the outlet air temperatures from AHU1 and AHU30 were achieved. Since these outlet air temperatures were similar, the pressure drops in all the branches were similar. Consequently, the pressure difference sensor can be placed anywhere. As the results for this fault show, the controllability of this system is still good.

In Figure 4, the PI_P for the fouled return pipes has both positive and the negative values, so it is difficult to label this index. The reason for this is that in the case of this fault, the pump head reaches the pump head maximum. Therefore, under the low cooling loads, the water flow rate is low, while the pump head can be high. In contrast, under the high cooling load at mid-day, the water flow rate should be high, while the pump head is also high. Since the pump head cannot be increased over the maximum, the flow rate is decreased, so the pump power appears to be decreased. The average daily value of the PI_P is higher than 10%. Therefore, the label for PI_P for this fault is P. This fault shows that additional performance indices should be involved for better fault detection, for example the pump head and the water flow rate.

The chosen fault parameters for fault modeling were chosen so that the PI values can resulted in significant values, as shown from Figures 4 to 7. Several tests with different fault parameters were performed, while an analysis of the method behavior with varying fault parameters was not performed.

Currently, for the suggested method for generating cause-effect rules, no qualitative statistical analysis of the obtained PIs has been implemented. Therefore, for some of the tested faults, for example fouled pipe in Figure 4, it is difficult to perform labeling.

Based on the PI biases in Figures 3 to 7, the PIs were labeled before the five fault diagnosis rules have been developed. These FDD rules are given in Table 1. As mentioned in the method of this study, the rules were developed in three steep, where the fault detection implies the performance indices labeling by P, N or NF. Subsequently, classification of the labeled PIs is fault diagnosis.

Table 1. The list of FDD rules

Faults \ PIs	PI_Q	PI_P	PI_{TAO1}	PI_{TAO30}
No fault, or it is not possible to diagnose them by these PIs	NF	NF	NF	NF
Fouled pipe line that consists most part if the flow circulation of AHU1	N	P	P	NF
Fault in the inlet sensor with a positive bias	P	P	NF	NF
Fault in the outlet sensor with a positive bias	P	P	N	N
Possible fault in the pump control or hydronic network	N	N	N	P

The above rules in Table 1 can be correct, as the baseline for the performance indices is a performance without faults. Therefore, an additional work in developing the performance baseline guideline is necessary.

The above faults affect energy consumption of both cooling coils and pump. Influence of each fault, listed in Table 1, on the daily energy consumptions is the following:

- Old valve gives increase in the daily energy consumption of the cooling coils of 2.2%, while the pump consumption is decreased by 3%;
- Fault due fouled return pipe decreases cooling coil consumption by 13.3%, while the pump consumption is increased by 8.8%;
- Fault in the inlet sensor increases daily energy consumption of the cooling coils by 27% and the pump consumption by 18.3%;
- Fault in the outlet sensor increases cooling coil energy consumption by 16.2% and pump consumption by 26.4%;
- Fault in the pump control increases the cooling coils consumption by 1% and the pump consumption by 4.2%.

Currently, multiple faults have not been examined. By testing new faults, new FDD rules can be established.

6 CONCLUSIONS

The suggested method for developing cause-effect, FDD, rules consists of three steps: testing different faults, calculating the performance indices, and classifying the observed PIs. Therefore, such method is simple. The lack of the analysis quality of the PIs is disadvantage of the suggested method. Therefore, a future study should enhance this method by involving a statistical qualification of the indices. In addition, including a sensitivity analysis on the amount of the fault parameters can be an extension of the study. Using the suggested method the FDD rules for five faults were developed.

The inaccurate measurement of the pressure difference and the fault in the control valve do not affect the AHU outlet air temperatures. The effect of the fouled return pipes is the increased outlet air temperature and the pump power consumption, while there is a decrease in the cooling energy consumption. Both faults in the inlet sensor and the outlet sensor increase the cooling coil rate and the pump rate.

Some faults do not affect all the observed system performances because the system is capable of overcoming such a fault and achieve the desired performances. Therefore, it is necessary to analyze additional performances so that a certain fault can be diagnosed.

The established FDD rules can be used as manual instructions for the building operators. In addition, these rules can be used as a framework for the automated FDD algorithms that can be directly programmed in the BEMS.

ACKNOWLEDGEMENT

The first author is grateful to the Department of Building Service Engineering at the Hong Kong Polytechnic University for advice in learning the TRNSYS platform.

REFERENCES

DABO, Natural Resources Canada, Canmet Energy Technology Center. Available from http://cetc-varennes.nrcan.gc.ca/en/b_b/bi_ib/p_p.html.

Haves, P., D. Claridge, and M. Lui. 2001. Report assessing the limitations of EnergPlus and SEAP with options for overcoming those limitations, *California Energy Commission Public Interest energy Research Program, HPCBS #E5P2.3T1*.

Haves, P., and S. K. Khalsa. 2000. Model-Based Performance Monitoring: Review of Diagnostic Methods and Chiller Case Study. *Published in the Proceedings for ACEEE 2000 Summer Study on energy Efficiency in Buildings, Efficiency and Sustainability, August 20-25, 2000, Asilomar Conference Center, Pacific Grove, Lawrence Berkeley National Laboratory, University of California.*

Hyvarinen, J., and S. Karki (Eds). 1996. Building Optimization and Fault Diagnosis Source Book. *IEA Annex 25, VTT, Finland*.

Ma Z., S. W. Wang, and W.Pau. 2008. Secondary loop chilled water in super high rise. *ASHRAE Journal*, 50: 42-52.

Pakanen, J.E., and T. Sundquist. 2003. Automation-assisted fault detection of an air-handling unit; implementing the method in a real building. *Energy and Buildings* (35): 193-202.

Salsbury, T.I., and R. Diamond. 1999. Model – Based Diagnostics for Air Handling Units. *Diagnostics for Commercial Buildings: Research to Practice, San Francisco*.

Song, Y.H., Y. Akashi, and J.J. Yee. 2008. A development of easy-to-use tool for fault detection and diagnosis in building air-conditioning systems. *Energy and Buildings* (40): 71-82.

Wang, S.W., and F. Xiao. 2004. AHU sensor fault diagnosis using principal component analysis method. *Energy and Buildings* (36): 147–160.

Wang, S.W., and X. Xinhua. 2007. Effects of alternative control strategies of water-evaporative cooling systems on energy efficiency and plume control: A case study. *Building and environment*, In Press.

Xu, X., S.W. Wang, and Z. Ma. 2008. Evaluation of plume potential and plume abatement of evaporative cooling towers in a subtropical region. *Applied thermal engineering*, 28: 1471–1484.

Yu, B., AHC van Paassen, and S. Riahy. 2003. Open window and defective radiator valve detection. *Building Service Engineering Research and Technology*, 24(2): 117–124.